Fretting fatigue analysis on nuclear fuel cladding tubes

Lichen Tang, Shurong Ding, Yongzhong Huo*

Department of Mechanics and Engineering Science, Fudan University.
220 Handan Road, Shanghai 200433, China.
* Corresponding author: yzhuo@fudan.edu.cn

Abstract

Grid-to-rod fretting failure due to fuel rod vibration remains as a significant cause of nuclear fuel failure in pressurized water reactors (PWRs). In order to carry out fretting fatigue tests to tube shaped specimens, a special designed apparatus was developed. The strain-life curve of the Zr-4 tube specimen under some given fretting contact pressure is obtained. It is found that the fatigue life of the Zr-4 tube under fretting contact conditions can be substantially lower than its life without fretting. The fretting wear scars and fatigue cracks were analyzed by microscope. The results show that the initial crack does not occur at the middle of the contact area where the wear depth reached the maximum, but at the edge of the initial contact area. where the amplitude of stress is confirmed to reach the maximum by FEM simulation. The position of crack nucleation can be predicted by half-length of the initial contact region and the slip displacement.

Keywords: Fretting fatigue test, Tube specimen, Nuclear fuel cladding tube, Fretting fatigue nucleation.

1. Introduction

Fretting is a special wear process that occurs at the contact area between two materials under loads and subject to minute relative motions by vibrations or some other forces. Fretting decreases the fatigue strength of materials operating under cycling stresses [1, 2]. The fretting fatigue phenomenon is very complex because there are too many factors that can affect the fretting behavior of materials [3]. A number of studies were taken to analyze the effects of various parameters on the fretting damage, such as the contact pressure [4-6], the amplitude of slip displacement [4], the coefficient of friction [5] and the nature of contact [7, 8]. For various materials, both experimental and numerical methods are taken to analyze the fretting damage [6, 9-11, 15]. Bridge-type fretting pads were used in many fretting fatigue experiments to produce contact in two places on each side of the specimen [6, 13, 14]. The pair of bridges and its load cell had to be hung on the specimen during the test by friction, thus a large clamping force and a flat contact were a must. Petiot [9] bolted one foot of the bridge to the end of the specimen and reduced the clamping force to a value of 100N. Similar apparatus were developed for the cases of point contact, such as cylinder-cross-cylinder and sphere-on-flat. The advantages of two arrangements of specimens and fretting bridges were discussed by Waterhouse [17].

Grid-to-rod fretting failure due to fuel rod vibration remains as a significant cause of nuclear fuel failure in pressurized water reactors (PWRs) [16]. The fuel rods are supported by the friction forces between the fuel rods and the springs or dimples of the grids in a fuel assembly as shown in Fig.1. When the reactor operates, the coolant flows through the surface of the fuel rods, and causes a flow-induced vibration (FIV) phenomenon, which is considered as the main driving force for fretting damage of the fuel rods. Fretting wear experiments of nuclear fuel cladding tubes were carried out by Kim [7] to study the effects of contact forces and slip displacements on fretting wear

under environment of air as well as water.

In this paper, both experimental and numerical researches are taken for fretting fatigue analysis on Zr-4 tube specimen. In section 2, fretting fatigue experiment device, design and results will be introduced. In section 3, a similar structure as experiment is analysis by FEM. Initial crack nucleation can be predicted.

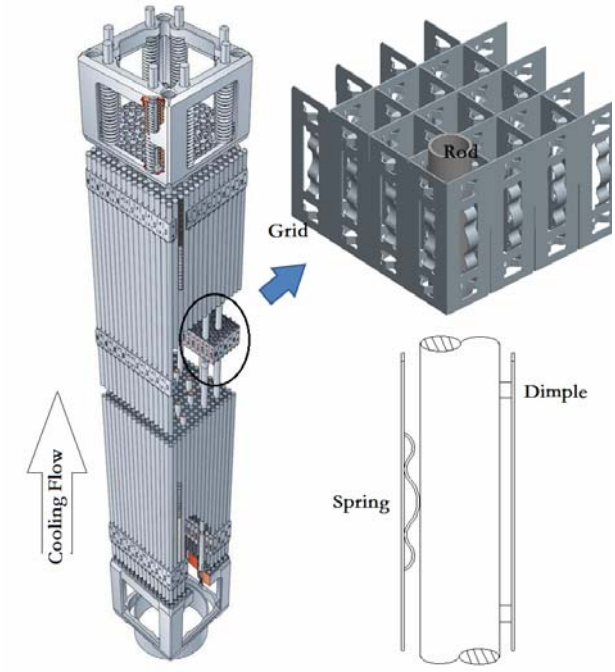

Figure 1. Grid-to-rod assembly

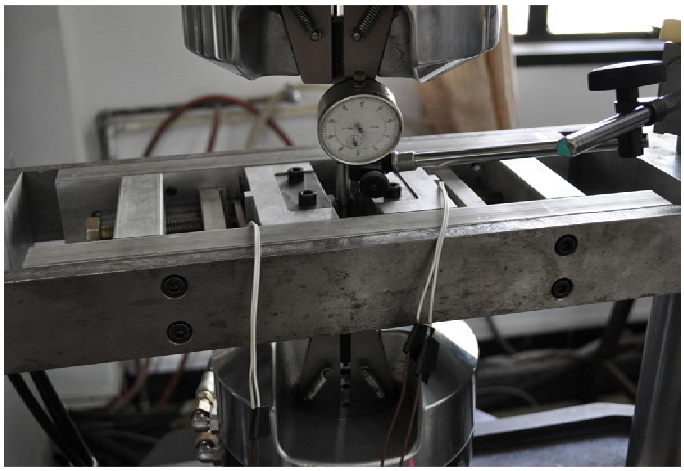

Figure 2. Fretting fatigue experiment device

2. Fretting Fatigue Experiment

2.1. Experiment Design

An experiment device is designed and added to a MTS fatigue testing machine, as shown in Fig. 2. It is assembled by several separated parts, and every part can be replaced for different experimental conditions. Compared with the bridge-type fretting apparatus, this kind of device is supported on the MTS machine directly but not hung on the specimen. A much smaller and stable contact force could be supplied. By using this device, fretting fatigue experiments can be made directly on tube specimens.

In our case, Zr-4 fuel rod cladding tubes (size Φ10mm×0.7mm×250mm) which are used in Chinese 300MWe reactors were tested as specimens. Its chemical composition is given in Table 1. As shown in Fig. 3, some necessary preventive measures were taken to make sure that there was no radial deformation neither any surface scars inside or outside the tube except the fretting point we expected. The contact force was set as 150N, and a constant amplitude displacement loading ($R_e=\varepsilon_{min}/\varepsilon_{max}$ =0.1) at a frequency of 10 Hz was applied. The contact geometry is a cylinder-cross-cylinder type. The pads are made of Cr12MoV Steel. The slip displacements (δ) between the pads and the specimen are determined by the imposed strain in specimen and the vertical motion of the pads during the tests measured by a dial indicator. For a maximum strain ε_{max} =0.4%, the slip displacement is 200 μm.

Table 1. Chemical composition of Zr-4 tube

Sn	Fe	Cr	O	Si	Al	C	Hf	N	Pb
1.30	0.22	0.11	0.13	0.0096	0.0051	0.0130	0.0053	0.0040	<0.0025

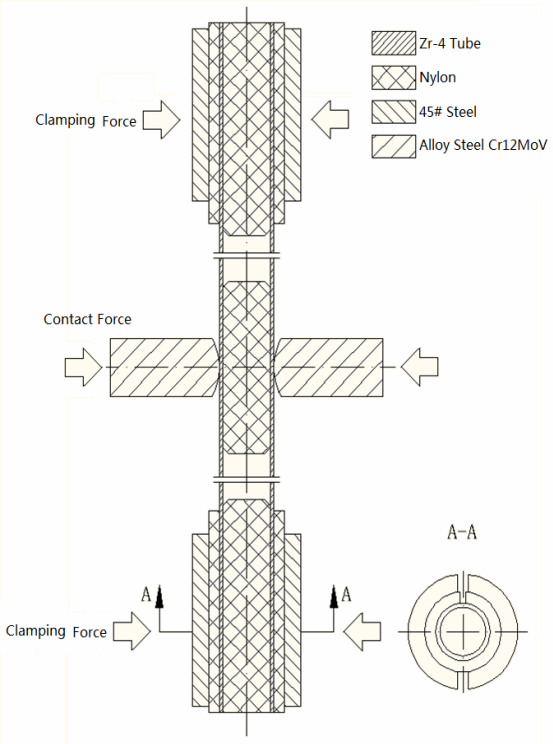

Figure 3. Geometry of assembled specimen

2.2. Experiment Results

Fig. 4 shows the fretting scars and cracks of two specimens for cases of maximum strain ε_{max}=0.6%. Ellipse fretting scars are made after 10^4 cycles. And the crack does not occur at the middle of the contact area where the wear depth reached the maximum, but at the edge of the initial contact area. Fig. 5 shows the comparison between fatigue S-N curve of the standard specimens and fretting fatigue S-N curve of the tube specimens. σ_{max} is the maximum engineering stress calculated by the measured force and the area of the section, σ_{min} is the minimum one, and $\Delta\sigma=\sigma_{max}-\sigma_{min}$ is the amplitude of the stress. N_f is the number of cycles when the specimen cracks. It is illustrated that the influence of fretting on the fatigue resistance occurs above 10^4 cycles and becomes stronger in higher cycle fatigue situation. The fretting decreases fatigue strength of material above 50% after 10^5 cycles. For cases of ε_{max}=0.4~0.8% (specimen no.6~15), the results are listed in Table 2. l_1 and l_2 is the length of the fretting scars on two sides of the specimen, and d_1 and d_2 are the corresponding distances from the crack to the middle of the fretting wear scar. The mean value of d equals 0.52834mm, and variance of d equals 0.0416mm^2.

Figure 4. Fretting scars and cracks of specimen no.9 and no.10

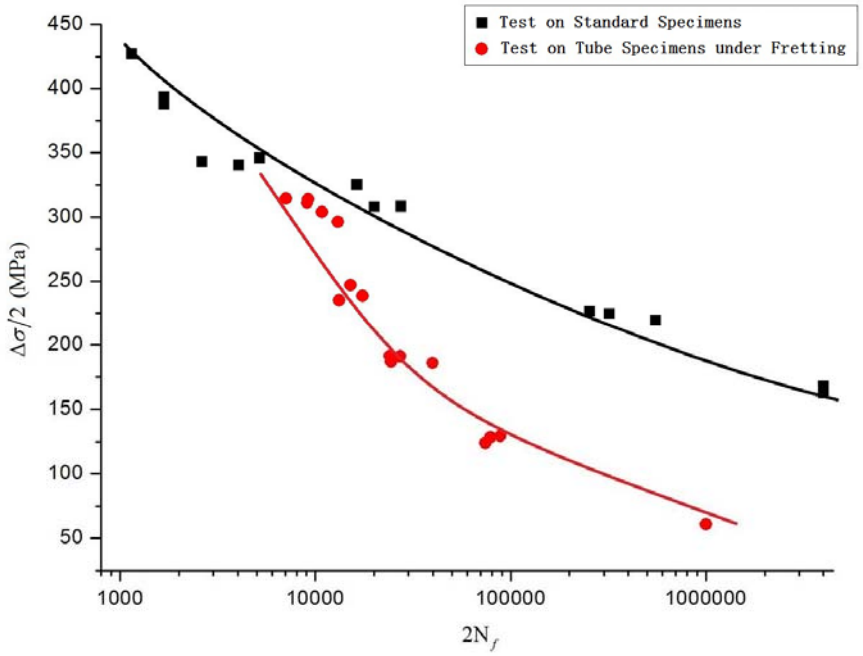

Figure 5. Comparison between fatigue S-N curve of the standard specimens and fretting fatigue S-N curve of the tube specimens

Table 2. Length of the wear scars and distance from the crack to the middle of the fretting wear scar

Specimen No.	l_1 (mm)	d_1 (mm)	l_2 (mm)	d_2 (mm)
6	2.3346	0.7933	2.4620	0.0726
7	2.6682	0.7525	2.3803	0.5883
8	2.4273	0.3545	2.3914	0.4456
9	2.4506	0.7165	2.5363	0.0740
10	2.5883	0.7197	2.5820	0.7666
11	2.5391	0.6570	2.4372	0.4760
12	2.7890	0.6986	2.5711	0.4131
13	2.2308	0.5218	2.3587	0.3494
14	2.2524	0.5993	2.1378	0.5708
15	2.3581	0.3850	2.2173	0.6122

3. FEM simulation

3.1 FEM model

Because of the symmetry of the structure, a quarter model of pad-on-tube structure is employed as shown in Fig. 6. The size of the tube is Φ10mm×0.7mm×100mm. Symmetrical boundary condition is applied on plane XoZ and XoY. Clamped boundary condition is applied on plane YoZ. P is the applied contact pressure on the back of the pad. Dload is the displacement load on the top end of the tube. Fig. 7 shows that the applied contact pressure keeps 7.5MPa during the displacement load

cycles and Dload with an range of 0.04~0.4mm is applied, which can make a similar fretting situation as the test (ε_{max} =0.4%, δ=200 μm, Re=0.1). Both tube and pad are considered as isotropic linear elastic material. The material parameters are listed in Table 3. Several cycles' loading is necessary because of plasticity.

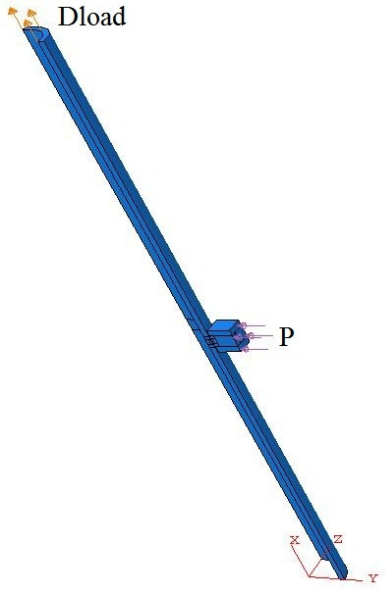

Figure 6. Quarter FEM model of pad-on-tube

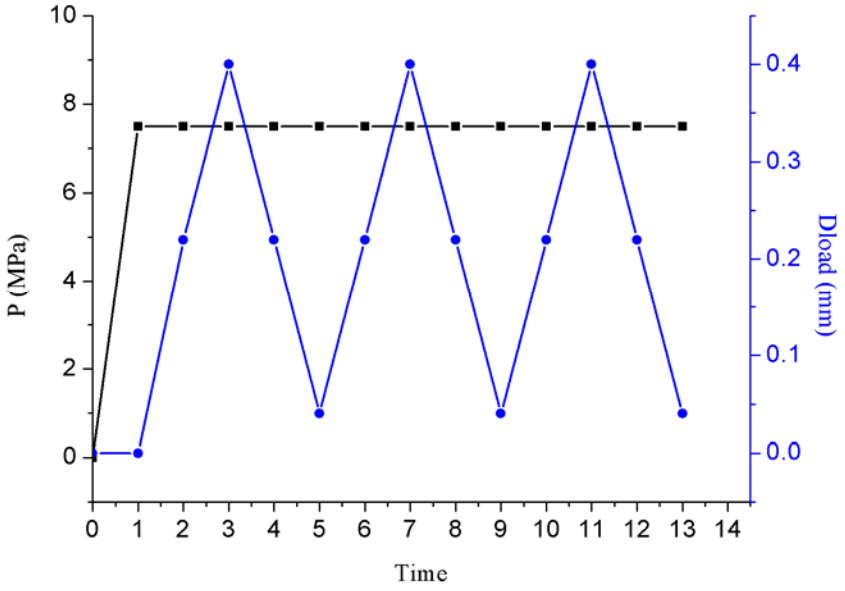

Figure 7. Applied contact pressure and displacement load

Table 3. Material Parameter

	Young's module	Passion's ratio
Tube	96GPa	0.43
Pad	206GPa	0.3

3.2 Simulation results

The contours of the contact pressure on the tube are plotted in Fig. 8 for different time steps. Fig. 8(a) shows that the initial contact region is an ellipse with a length of 600μm and a width of 480μm. Comparison of Fig. 8(a) and 8(b) shows that the contact region is moving with the increasing of the applied load. Fig. 9(a) and 9(b) shows the contact shear stress on the tube surface for the same Dload, but one is increasing and the other is decreasing. It is illustrated that the absolute value of the contact shear stress for the two cases are almost the same, but the directions of the friction force are the opposite. The contact pressures of path 1 for different times are shown in fig. 10. The contact region on the surface of the tube can be separated into two parts. One is always under the contact (noted as Region I in Fig. 10) and the other is scanned by the edge of the contact region during the cycles (noted as Region II in Fig. 10). The rest region of the tube surface is not under contact during the cycles (noted as Region III in Fig. 10). The separation of the contact surface is shown in fig. 11. σ_x is a periodic function with a same frequency of applied load. σ_x of three point from these three separated regions are shown in Fig.12. σ_x of point A keeps increasing in the loading process and decreasing in the unloading process. For the point B, the increasing of σ_x in the loading process is faster than in region I and reaches a maximum value when the edge of the contact region scans over it. And the decreasing of σ_x in unloading process is also faster than point A and reaches a minimum

value when the edge of the contact region scans over it again. For the point C, σ_x keeps negative during the loading and unloading process. Apparently, the amplitude of σ_x of the point B is much larger than the point A and the point C because of the scanning of the contact edge.

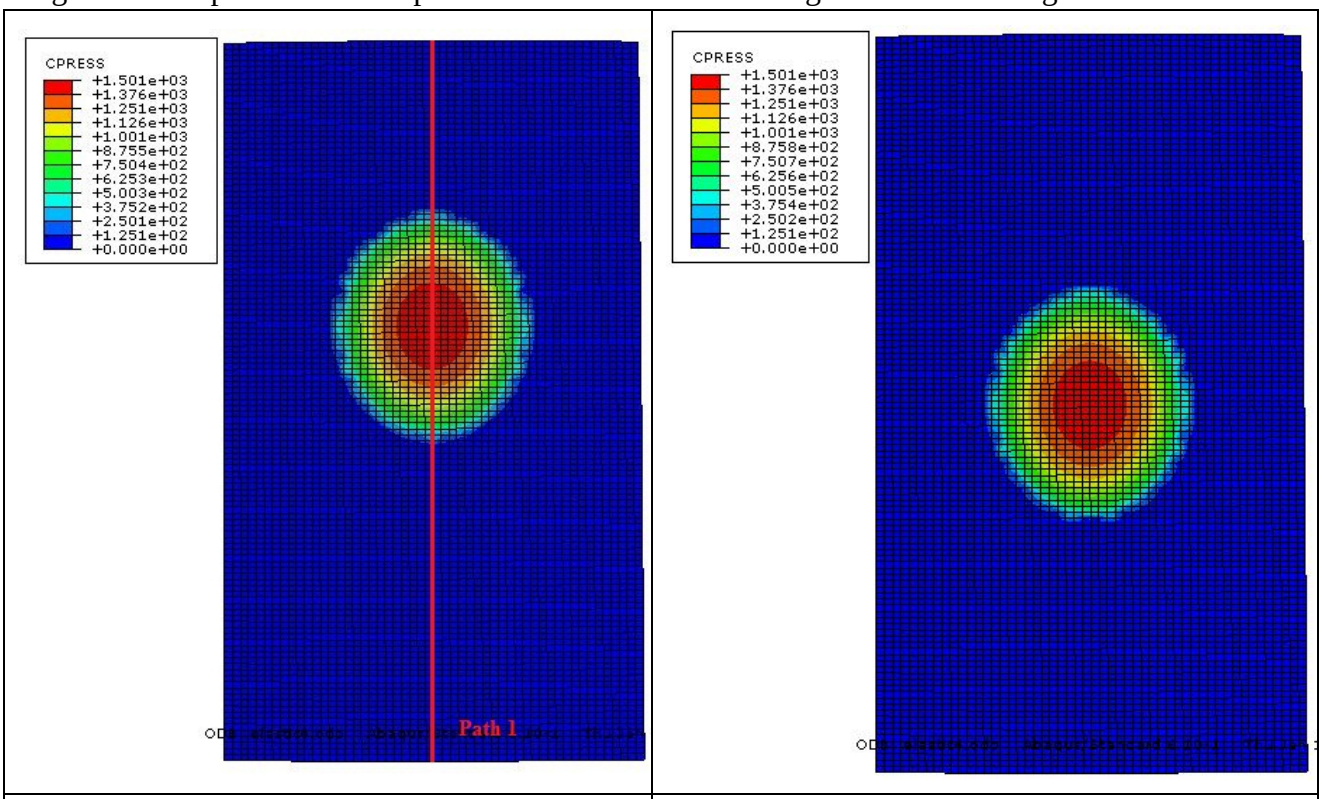

(a) (b)

Figure 8. Contact pressure on the tube surface for (a)time=1.0; (b)time=3.0

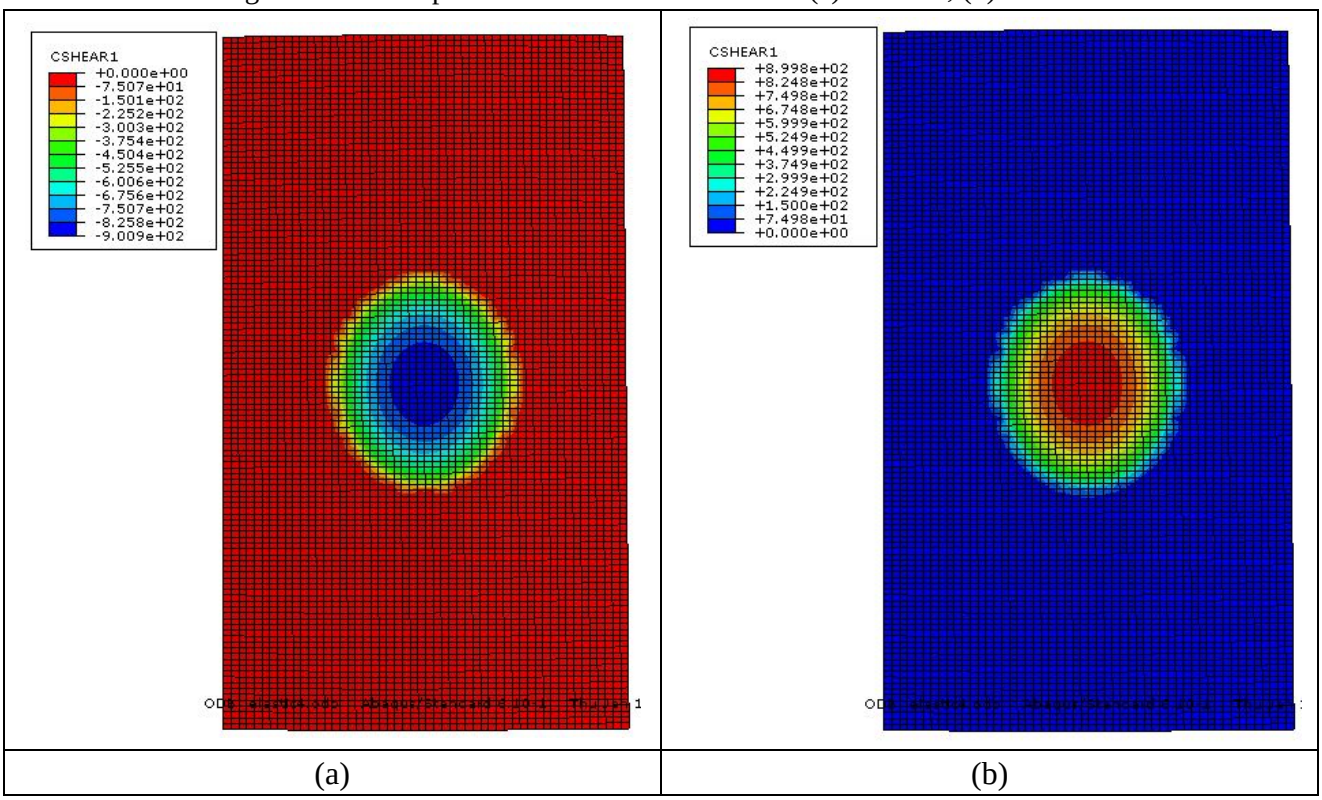

(a) (b)

Figure 9. Contact shear stress on the tube surface for (a) time=2.9; (b) time=3.1.

σ_{max} and σ_{min} are of path 1 are shown in Fig. 13, where

$$\sigma_{max}(x) = \max_t(\sigma_x(x,t)), \qquad \sigma_{min}(x) = \min_t(\sigma_x(x,t)), .$$

It is illustrated that the σ_{max} of nodes in region II are larger than the nodes in region I and region III. σ_{max} reaches a maximum value when the contact region moves to the red region in Fig. 11 because of the cumulated effect of contact shear stress and maximum applied load. $\Delta\sigma = \sigma_{max} - \sigma_{min}$ is shown in Fig. 14. It gives a different property with the stress amplitude of a standard specimen as shown in Fig 15. It may clarify that the crack does not occur at the middle of the contact area where the wear depth reached the maximum, but at the edge of the contact area.

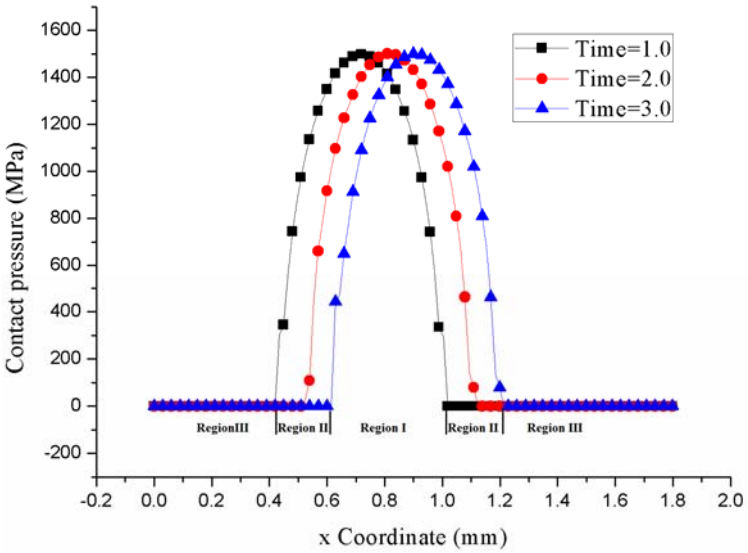

Figure 10. The contact pressures of path 1 for different times.

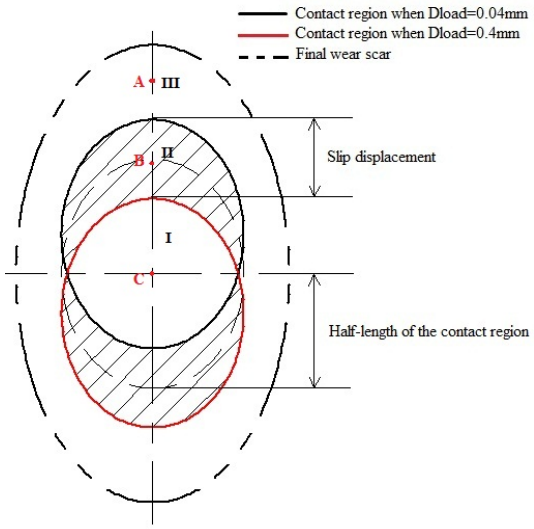

Figure 11. The regions on the surface of the tube.

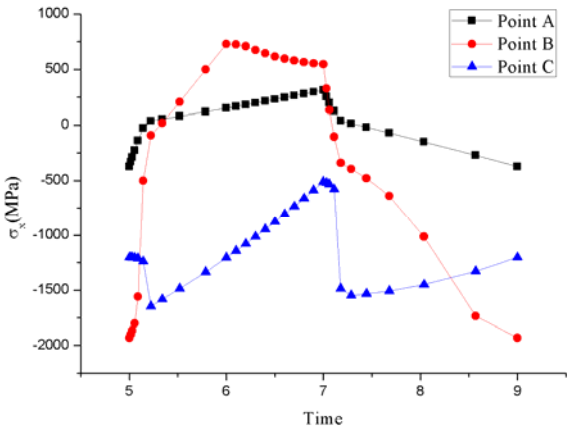

Figure 12. Stress of the elements in the three different regions

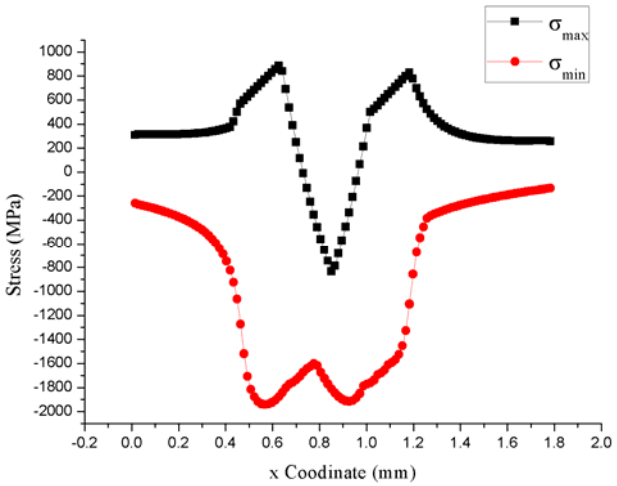

Figure 13. The maximum and minimum stress of nodes on path 1 during one cycle.

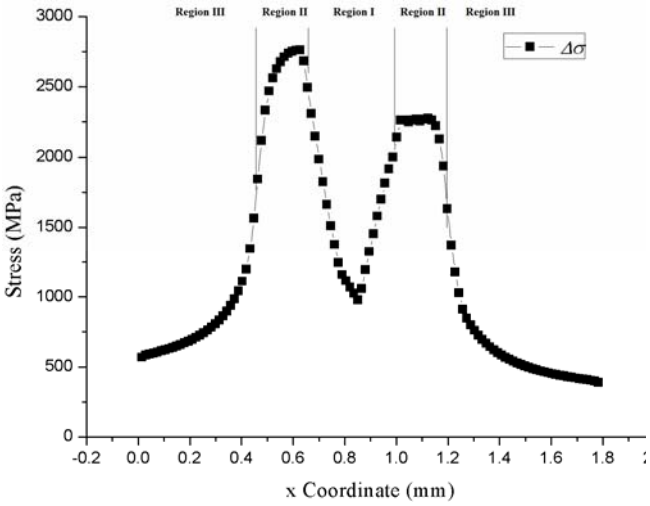

Figure 14. The stress amplitude of nodes on path 1 during one cycle.

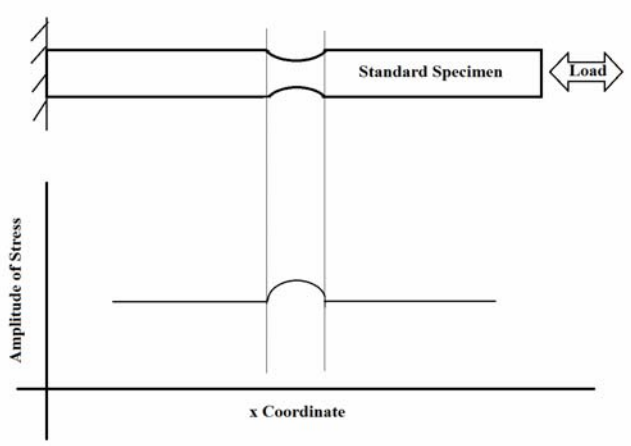

Figgure 15. The stress amplitude of a standard specimen.

4. Conclusion and discussions

(1) The fretting fatigue experiment taken on tube specimen gives a S-N curve of nuclear fuel cladding tube material. It is illustrated that the influence of the fretting on the fatigue resistance occurs above 10^4 cycles and becomes stronger in higher cycle fatigue situations. The fretting decreases fatigue strength of material above 50% after 10^5 cycles.

(2) The fretting fatigue experiment shows that crack does not occur at the middle of the contact area where the wear depth reached the maximum, but at the edge of the initial contact region. The mean value of distances from the crack to the middle of the fretting wear scar (d) equals 0.52834mm, and variance of d equals 0.0416mm^2.

(3) An FEM simulation is employed to analyze the crack nucleation on the tube surface. It is predicted that the region scanned by the edge of the contact region during the cycles will be the region of crack nucleation. The region II in Fig. 10 can be predicted by initial contact region and slip displacement. The distance from the crack to the middle of the fretting wear scar $d=a\pm\delta/2$, where a is the half-length of the initial contact region.

(4) Elastic materials are used in this simulation, which leads a smaller contact region and a larger contact stress. For the case in Section 3.1, a=0.455mm and δ=0.2mm if linear elastoplastic materials are employed in the simulation. This fits the tests of the specimen no.13~15 better.

Acknowledgements

This work was supported by the National Natural Science Foundation of China(No.11072062, 11172068 and 11272092), the Research Fund for the Doctoral Program of Higher Education of China (20110071110013), the High Technology Develop Program of China (863 Program: 2009AA04Z408) and the Graduate Innovation Fund of Fudan University.

References

[1] P.L. Hurricks, Mechanism of fretting. Wear, 15 (1970) 389-409.

[2] R.B. Waterhouse, Fretting fatigue. International Materials Reviews, 37(1992) 77-98.
[3] J.M. Dobromirski, Variables of fretting process: are there 50 of them? AETM STP 1159, American Society for Testing and Materials, Philadelphia, 1992,pp. 60-66.
[4] H. Mohrbacher, J.P. Celis, J.R. Roos, Laboratory testing of displacement and load induced fretting. Tribology International, 28(1995) 269-278.
[5] H.A. Fadag, S. Mall, V.K. Jain, A finite element analysis of fretting fatigue crack growth behavior in Ti-6Al-4 V. Engineering Fracture Mechanics, 75(2008) 1384-1399.
[6] N.K.R. Naidu, S.G.S. Raman, Effect of contact pressure on fretting fatigue behaviour of Al-Mg-Si alloy AA6061. International Journal of Fatigue, 27(2005) 283-291.
[7] H.K. Kim, Y.H. Lee, S.P. Heo, Mechanical and experimental investigation on nuclear fuel fretting. Tribology International, 39(2006) 1305-1319.
[8] J.A. Pape, R.W. Neu, Influence of contact configuration in fretting fatigue testing. Wear, 225-229(1999) 1205-1214.
[9] C. Petiot, et al. An analysis of fretting-fatigue failure combined with numerical calculations to predict crack nucleation. Wear, 181-183(1995) 101-111.
[10] A.L. Hutson, T. Nicholas, R. Goodman. Fretting fatigue of Ti-6Al-4V under flat-on-flat contact. International Journal of Fatigue, 21(1999) 663-669.
[11] J.M. Wallace, R.W. Neu. Fretting fatigue crack nucleation in Ti-6Al-4V. Fatigue Fract Engng Mater Struct, 26(2003)199-214.
[12] M.P. Szolwinski, T.N. Farris. Mechanics of fretting fatigue crack formation. Wear, 198(1996) 93-107.
[13] T. Hattori, M. Nakamura, et al., Simulation of fretting-fatigue life by using stress-singularity parameters and fracture mechanics. Tribology International, 36(2003) 87-97.
[14] Y. Liu, J.Q. Xu, Y. Mutoh, Evaluation of fretting wear based on the frictional work and cyclic saturation concepts. International Journal of Mechanical Sciences, 50 (2008) 897-904.
[15] D.A. Hills, Mechanics of fretting fatigue. Wear, 175(1994) 107-113.
[16] W. Klinger, IAEA-TECDOC-1345, 2002, pp 21-29.
[17] R.B. Waterhouse. The Problems of Fretting Fatigue Testing, Standardization of Fretting Fatigue Test Methods and Equipment, ASTM STP 1159. American Society for Testing and Materials, Philadelphia, 1992: 13-19.